NEGATIVELY BUOYANT DEBRIS IMPACT UNDER TSUNAMIS-LIKE CONDITIONS

Jaril Deschamps, Institut National de la Recherche Scientifique, jaril.deschamps@inrs.ca
Jacob Stolle, Institut National de la Recherche Scientifique, jacob.stolle@inrs.ca
Damien Pham Van Bang, École de Technologie Supérieure, damien.pham-van-bang@etsmtl.ca

BACKGROUND

Field surveys following major coastal disasters, such as the Chile tsunami in 2010 or the Tohoku tsunami in Japan in 2011, have pointed out the lack of resilience of coastal communities to such events and the need to better understand the risks associated with them (Takahashi et al. [2010]; Palermo et al. [2013]; Esteban et al. [2015]). While the primary cause of destruction during tsunamis remains associated with the hydraulic loads (hydrostatic, hydrodynamics, wave impact, etc.), it has been demonstrated that debris loading is also a major cause of damage on structures, mainly through debris impact and damming (Yeh et al. [2014]). In the past decade, multiple studies have addressed debris transport and loading in extreme events (Shafiei et al. [2016]; Ikeno et al. [2016]; Stolle et al. [2018]). However, those studies mainly focused on positively buoyant debris, like wood logs or empty containers, leaving a gap in knowledge. Indeed, Stolle et al. [2020], in a field survey following the Indonesian tsunami in 2018, identified the study of neutrally and negatively buoyant debris as one of five major needs in debris loading research, with even ASCE7-16 Chapter 6 containing limited recommendation on the load associated with those type of debris.

The impact force has generally been estimated using the single degree-of-freedom rigid impact equation given by Haehnel and Daly [2004]:

$$F_{i,max} = u_d\sqrt{\hat{k}\left(m_d + Cm_f\right)} \qquad (1)$$

Where $F_{i,max}$ is the maximum impact force, u_d the debris impact velocity, $\hat{k}$ the effective stiffness of the collision, m_d the debris mass, C the added mass coefficient and m_f the displaced fluid mass.

Based on Eq.1, negatively buoyant debris will act differently from positively buoyant debris in mainly two ways. First, with a higher degree of submergence, added mass should have an influence for negatively buoyant debris (Stolle et al. [2020]), which would result in a higher impact magnitude. Secondly, with transportation modes different from positively buoyant debris, such as saltation, rolling and sliding (Imamura et al. [2008]), negatively buoyant debris should interact more with the bed, reducing their final velocity which is often considered equal to that of the bore wave (Shafiei et al. [2016]).

To address this hypothesis, small scale experiments were conducted with negatively buoyant debris at the Institut National de la Recherche Scientifique (INRS), in Québec, Canada.

OBJECTIVES

This study aims to contribute to the development of improved construction guidelines in the coastal zone. More precisely, the primary objectives of this study were to:

1. Study the influence of debris density, added mass, and debris material on maximum impact loads.
2. Compare conclusions with positively buoyant debris studies.
3. Propose an equation incorporating the influence of debris buoyancy on impact loads.

EXPERIMENTAL PROGRAM

The experiments were conducted in a 9.0 m long by 0.3 m wide wave flume. The tests consisted of generating a bore wave using a dam-break wave mechanism that would then transport a single debris toward a cylindrical structure. Tests were conducted at a 1/60 scale. Three different reservoir heights [*h*] were used to generate the bore waves: 0.17 m, 0.22 m, and 0.27 m. This resulted in a maximum wave height [*H*] at the structure of approximately 0.02 m, 0.04 m, and 0.06 m. Figure 1 provides more details on the experimental set-up.

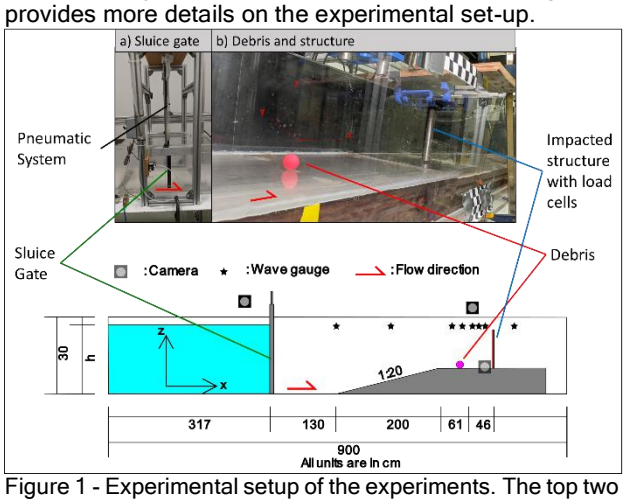

Figure 1 - Experimental setup of the experiments. The top two pictures are of the actual setup, and the bottom displays a more detailed diagram of the system.

The structure itself consisted of a cylindrical stainless-steel rod with a 0.0254 m diameter. This cylinder was attached to 2 load cells through a guidance system allowing it to move freely in the XY plane. The load cells, positioned in the X and Y axis, were both sampling at 6 kHz and had a load range of ±2230 N.

The debris were homogenous spheres. Four diameters of debris [d_d] (0.0127 m, 0.0159 m, 0.019 m, and 0.0254 m) and 6 different materials were used, resulting in 24 different debris. Table 1 give more details about the debris material properties.

Table 1 – Properties of the different debris materials used.

MATERIAL	PP	NYLON	ACRYLIC	DELRIN	PTFE	STAINLESS STEEL
RELATIVE DENSITY	0.90	1.14	1.19	1.42	2.15	7.80
YOUNG'S MODULUS [*E*] (GPA)	1.10-1.60	1.60-3.80	2.70-3.30	2.5-4.0	0.40-0.80	190-200

In total, 72 different configurations were tested, each configuration being repeated at least three times.

RESULTS AND DISCUSSION

Similar to previous studies, debris final velocities were consistently smaller than the front bore velocity, with a decreasing velocity as size (and mass) increased for stainless steel debris. Figure 2 presents a comparison between debris velocity and bore velocity for a reservoir depth of 0.27 m. The larger, heavier debris tended to interact more with the bed resulting in the further reduced velocity.

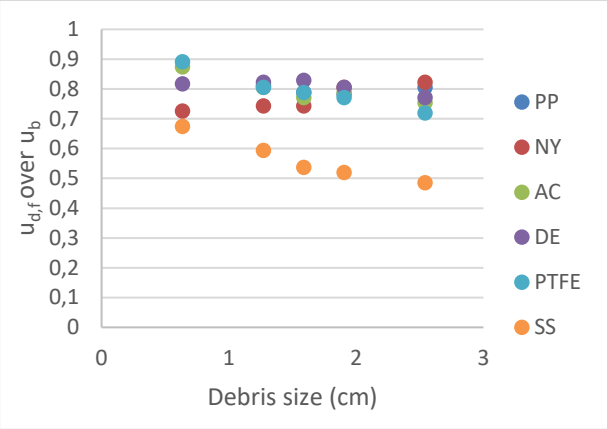

Figure 2 – Rate of the final debris velocity [$u_{d,f}$] over the front bore velocity [u_b] in relation to the debris size, with a reservoir depth of 0.27 m

Preliminary results put the maximum response force of the structure with the debris mass, size and material. Figure 3 shows this relation. As expected, increased debris mass led to higher impact force.

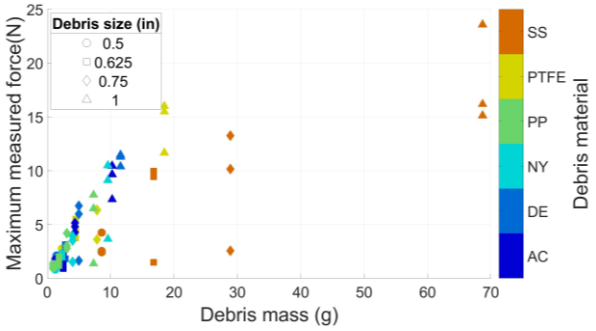

Figure 3 – Relationship between structure response force and different debris properties, with a reservoir depth of 0.27 m.

CONCLUSION AND NEXT STEPS

This study presents one of the first experimental programs to analyze the impact magnitude of negatively buoyant debris on structures. Seventy-two different configurations of debris size, debris material, and bore height were tested, allowing for a precise analysis of each parameter. Furthermore, a direct comparison with positively buoyant debris was performed in conjunction which enabled a validation of the experimental results with those of previous studies. Preliminary results show that negatively buoyant debris tend to interact more with the ground, leading to a smaller final velocity. Further analysis will allow to extract velocity trends and link them to the debris and wave properties. Additionally, the impact force will be extracted from the impact response by correlating the structural response to known impacts. Separating the impact magnitude and structure response will allow for a deeper understanding of the processes and the development of an impact equation incorporating debris density.

REFERENCES

ASCE (2016): Minimum design loads for buildings and other structures. American Society of Civil Engineers, Virginia, USA. doi:10.1061/9780784412916.

Esteban, M., H. Takagi, and T. Shibayama (2015.): Handbook of Coastal Disaster Mitigation for Engineers and Planners.

Haehnel, R. B., and Daly, S. F. (2004): Maximum impact force of woody debris on flood-plain structures. J. Hydraul. Eng., 10.1061/(ASCE)0733-9429(2004)130:2(112), 112-120.

Ikeno, M., Takabatake, D., Kihara, N., Kaida, H., Miyagawa, Y., Shibayama, A. (2016): Improvement of collision force formula for woody debris by airborne and hydraulic experiments. Coast Eng. J. 58, 1640022.

Imamura, F., Goto, K., Ohkubo, S. (2008): A numerical model for the transport of a boulder by tsunami. J. Geophys. Res. 113, C01008 https://doi.org/10.1029/2007JC004170.

Palermo, D., I. Nistor, M. Saatcioglu, and A. Ghobarah (2013): Impact and damage to structures during the 27 February 2010 Chile tsunami. Canadian Journal of Civil Engineering 40:750-758.

Shafiei, S., et al. (2016): Measurements of tsunami-borne debris impact on structures using an embedded accelerometer. Journal of Hydraulic Research 54(4): 435-449.

Stolle, J., et al. (2018): Debris impact under extreme hydrodynamic conditions part 2: Impact force responses for non-rigid debris collisions. Coastal Engineering 141: 107-118.

Stolle, J., et al. (2020): Engineering lessons from the 28 September 2018 Indonesian tsunami: debris loading. Canadian Journal of Civil Engineering 47(1): 1-12.

Takahashi, S., T. Sugano, T. Tomita, T. Arikawa, D. Tatsumi, H. Kashima, S. Murata, Y. Matsuoka, and T. Nakamura (2010): Joint survey for 2010 Chilean earthquake and tsunami disaster in ports and coasts. Port and Airport Res Inst.

Yeh, H., A. R. Barbosa, H. Ko, and J. G. Cawley (2014): TSUNAMI LOADINGS ON STRUCTURES: REVIEW AND ANALYSIS. Coastal Engineering Proceedings 1:currents-4.